



Scientific Research Report

Deep Learning-Based Detection of Periodontal Infrabony and Furcation Defects on Periapical Radiographs: A Feasibility Study

Nicola Alberto Valente^{a,b*}, Lorenzo Maria Americo^a, Fabrizio Ciancetta^c, Simone Mari^{a,c}

^a Division of Periodontics, School of Dental Medicine, Department of Surgical Sciences, Faculty of Medicine, University of Cagliari, Cagliari, Italy

^b College of Dentistry, American University of Iraq Baghdad (AUIB), Baghdad, Iraq

^c Department of Industrial and Information Engineering and Economics, University of L'Aquila, L'Aquila, Italy

ARTICLE INFO

Article history:

Received 10 October 2025

Received in revised form

8 December 2025

Accepted 21 December 2025

Available online xxx

Key words:

Infrabony Defects

Periodontal Defects

Deep Learning

Artificial Intelligence

Diagnostic Imaging

ABSTRACT

Introduction: Accurate radiographic detection and classification of periodontal osseous defects are essential for prognosis and surgical planning in regenerative periodontology. Traditional diagnostic methods offer limited morphological information, and interpretation can be operator-dependent. Recent advances in artificial intelligence (AI) have shown potential in medical image analysis, but their application to detailed classification of periodontal defects on periapical radiographs remains underexplored.

Methods: A total of 7464 periapical radiographs were retrospectively collected from the clinical archive of the University Hospital of Cagliari. After expert annotation, 581 images containing at least 1 periodontal osseous defect were included. Defects were categorised into 4 types: 1-wall defects, 2-or-more-wall defects, crater-like defects, and furcation involvements. A YOLOv8 large (YOLOv8l) object detection model was trained using a patient-independent split (406 trainings, 58 validations, 117 testings). Performance was assessed using mean Average Precision (mAP) at IoU thresholds of 0.5 and 0.5:0.95, as well as class-wise precision and recall.

Results: The model achieved an overall precision of 0.592, recall of 0.435, and mAP@0.5 of 0.504. Furcation involvements showed the highest precision (0.669) and mAP@0.5 (0.577), followed by crater-like defects and multi-wall defects. One-wall defects were the most difficult to detect. Qualitative analysis revealed that smaller or radiographically ambiguous defects were more frequently missed.

Conclusions: AI-assisted object detection demonstrated feasibility in classifying periodontal defects, but current performance remains limited. Although current performance is limited by dataset imbalance and the inherent constraints of 2D imaging, these models may enhance diagnostic consistency and support treatment planning.

Clinical relevance: This study demonstrates the feasibility of using an AI-based object detection model to classify such defects on standard periapical radiographs. By supporting clinicians in the radiographic interpretation of defect morphology, the proposed system may contribute to more consistent diagnoses, improved case selection, and enhanced predictability of surgical outcomes in periodontal therapy.

© 2025 The Authors. Published by Elsevier Inc. on behalf of FDI World Dental Federation.

This is an open access article under the CC BY-NC-ND license

(<http://creativecommons.org/licenses/by-nc-nd/4.0/>)

* Corresponding author. Division of Periodontics, School of Dental Medicine, Department of Surgical Sciences, Faculty of Medicine, University of Cagliari, Cittadella Universitaria snc, Blocco I, Monserrato CA 09042, Italy

E-mail address: nicola.valente@unica.it (N.A. Valente).

<https://doi.org/10.1016/j.identj.2025.109380>

0020-6539/© 2025 The Authors. Published by Elsevier Inc. on behalf of FDI World Dental Federation. This is an open access article under the CC BY-NC-ND license (<http://creativecommons.org/licenses/by-nc-nd/4.0/>)

Introduction

The treatment of periodontal intrabony defects has long posed a clinical challenge. Before the advent of regenerative techniques, therapeutic strategies relied on resective or

access flap surgery, aiming primarily at pocket reduction rather than reconstruction of lost attachment.¹⁻³ In a seminal 1967 report, the anatomical complexity of vertical bone defects and the limited healing capacity of conventional approaches were described.⁴ The paradigm shifted in the 1980s with the biological framework proposed by Melcher and the histologic studies by Nyman et al., which demonstrated that selective repopulation of the wound by periodontal ligament cells could lead to true regeneration of the attachment apparatus.^{5,6}

Over the last 3 decades, clinical trials and reviews have established the efficacy of regenerative therapies, such as guided tissue regeneration, enamel matrix derivatives, and bone grafts, in achieving new bone, cementum, and periodontal ligament formation.⁷⁻¹⁴ However, regenerative outcomes are strongly influenced by defect morphology. Narrow, deep, and containing defects offer a predictable environment for regeneration, whereas wide, shallow, or 1-wall defects are less responsive.¹⁵⁻¹⁷ Thus, accurate characterisation of defect anatomy is essential for case selection, prognosis, and surgical planning.

Traditional assessment of defect morphology relies on clinical probing and intraoperative findings, with limited predictive value from standard radiographs. Yet, radiographs remain the most commonly used diagnostic tool in daily periodontal practice. This gap between clinical need and diagnostic capacity presents an opportunity for artificial intelligence (AI)-based solutions. Object detection models have demonstrated promising performance in real-time medical image analysis, balancing accuracy and speed.¹⁸⁻²¹

In recent years, studies have investigated the application of machine learning models in periodontology, particularly for the radiographic detection of periodontal bone loss. Most of these efforts have focused on panoramic radiographs, leveraging their wide anatomical coverage for automated assessment of periodontal status. A more limited number of studies have explored the use of periapical radiographs, which provide greater detail at the site level and are more commonly used in daily periodontal diagnostics.²²⁻²⁴ Building upon this growing body of research, it would be relevant to explore whether deep learning-based object detection approaches can effectively address the classification of periodontal osseous defects on intraoral radiographs. Previous AI studies have addressed periodontal bone loss detection (often on panoramic X-rays or focusing on single defect types); here we extend this work by using periapical radiographs for detailed classification of individual defect morphologies.^{23,24} In routine periodontal practice, the initial diagnostic imaging relies on a full-mouth series of 2D periapical radiographs. Consistent with the ALARA (As Low As Reasonably Achievable) principle, CBCT is considered a second-level exam and is not routinely indicated at the initial periodontal assessment. Our study, therefore, focuses on the radiographic scenario that clinicians commonly face in daily care.

The present study aims to explore the feasibility of developing an AI-based model for the automatic detection and classification of periodontal infrabony and furcation defects on intraoral radiographs. By leveraging deep learning techniques, the study seeks to assess whether clinically relevant bony defects can be identified and categorised according to

their morphology using standard periapical imaging. Such a tool could support clinical decision-making by providing objective, reproducible diagnostic information, potentially improving case selection and treatment planning in regenerative periodontology.

Materials and methods

This study was approved by the Territorial Ethics Committee of Sardinia (RAS A00 12-01-00 Prot. n. 18698, session no. 48 of June 24, 2025) and has been registered at ClinicalTrials.gov NCT07086625. All procedures were conducted in accordance with the Declaration of Helsinki and reported according to the 2024 CLAIM (Checklist for Artificial Intelligence in Medical Imaging) reporting guidelines.²⁵

The study followed a cross-sectional, diagnostic design and consisted of 2 main phases: (1) the development and training of an AI model for the automatic detection of periodontal osseous defects, and (2) its validation on an independent clinical dataset.

The available training dataset was composed of 7464 intraoral periapical radiographs retrospectively collected from the clinical archive of the Dental Clinic of the University Hospital of Cagliari. Out of 7464 collected radiographs, only 581 images that contained at least one identifiable infrabony or furcation defect were ultimately included for model training and evaluation. The retrospective use of archived intraoral radiographs for model development and testing was possible in accordance with Article 9(2)(j) and Article 89 of the General Data Protection Regulation (GDPR, EU 2016/679), and with Article 110 of the Italian Legislative Decree 196/2003, as amended by Legislative Decree 101/2018, given the large number of patients, the retrospective nature of data collection and the objective impossibility to recontact individuals to obtain specific consent. To this end, all radiographic data were fully anonymised prior to analysis, with the removal of any direct or indirect identifiers and implementation of technical and organisational measures to prevent re-identification.

The study was conducted in full compliance with data minimisation principles (Article 5.1.c GDPR) and with the security, anonymisation, and accountability requirements of Articles 24, 25, and 32 of the GDPR. The exclusive purpose of data processing was scientific research in the public interest, specifically aimed at improving diagnostic workflows in periodontology through AI-based image analysis.

Data sources and annotation

Annotation of the images was performed by 2 experienced periodontists with over 10 years of clinical and academic experience in the diagnosis and treatment of periodontal disease. The experts independently reviewed the radiographs and identified periodontal defects according to well-defined morphological criteria. Four categories were considered: vertical defects with a single remaining wall, vertical defects with 2 or more remaining walls, interproximal craters, and furcation involvements. Annotation was conducted using only the radiographic appearance of the defect, without

access to clinical charts or surgical documentation, in order to reflect real-world diagnostic conditions based solely on imaging.

To promote consistency, the annotators were calibrated through a preliminary review of a subset of 50 images, during which labeling criteria and interpretation guidelines were jointly discussed. For the main dataset, each image was independently annotated by both experts using the LabelImg software (Free software: MIT license, Tzutalin. LabelImg. Git code (2015). <https://github.com/tzutalin/labelImg>), which allowed for precise bounding box placement around the areas of interest, thus generating a structured dataset for supervised model training. In cases of disagreement between annotators, the final label was established through consensus discussion. No third reviewer was required.

After image annotation, a total of 7464 intraoral radiographs were available for review. Among these, 581 images were identified as containing at least one periodontal bone defect and were therefore included in the development and evaluation of the AI model.

To ensure robust model training and evaluation, the dataset was divided into 3 subsets: training, validation, and test sets. The split was stratified to maintain a representative distribution of the 4 defect categories (1-wall defects, 2-or-more-wall defects, crater-like defects, and furcation involvements) and to prevent any overlap of patient data between subsets.

Table 1 – Distribution of images and instances per class in the training, validation, and test sets

Class	Train (images/instances)	Validation (images/instances)	Test (images/instances)
1	58/63	12/12	17/18
2+	220/246	26/29	55/59
Crater	89/93	16/17	26/27
Furcation	96/100	11/12	33/33
Total	406/502	58/70	117/137

1: 1 wall defect; 2+: 2 or 3 walls defects; Crater: crater-shaped interproximal bone resorption; Furcation: furcation defects.

The final allocation consisted of 406 images for training, 58 for validation, and 117 for testing. Each image could contain one or more annotated defects, as detailed in Table 1.

This stratified division allowed for both effective model learning and an unbiased assessment of performance on previously unseen data. The training set was used to optimise model parameters, the validation set to monitor learning and prevent overfitting, and the test set to provide an independent evaluation of the model's ability to detect and classify periodontal bone defects across all 4 clinically relevant categories (Figure 1).

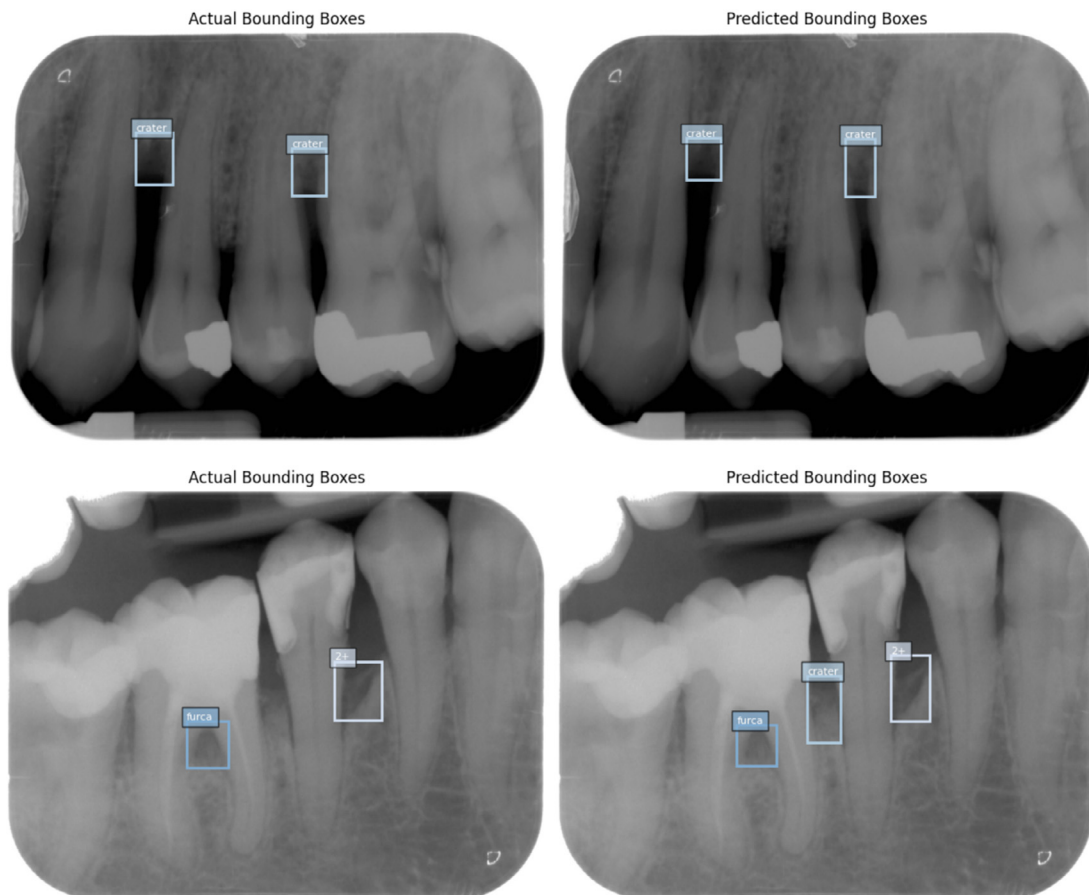


Fig. 1 – Comparison of actual and predicted bounding boxes for periodontal defects in radiographic images. The left panels display the ground truth bounding boxes for each defect, while the right panels show the bounding boxes predicted by the model.

For the training phase, the YOLOv8 (Ultralytics Inc.) model in its large variant (YOLOv8l) was selected—a state-of-the-art convolutional neural network optimised for object detection. The architecture includes a backbone for feature extraction, a neck for the fusion of spatial and semantic information, and a head for class and bounding box prediction. YOLOv8l is an open-source model. Training was conducted on images standardised to a resolution of 640×640 pixels, with a batch size of 16 and optimisation via AdamW (learning rate 0.00125). Data augmentation techniques (including rotations, translations, and variations in brightness and contrast) were employed to increase dataset variability and improve the model's generalisation capability. The process was executed on high-performance hardware (NVIDIA GeForce RTX 4090 GPU), utilising mixed precision to optimise computational efficiency and speed. Advanced interpretability tools were not employed; however, a visual overlay of the model's predictions on the radiographs was provided, which is considered a minimal and accepted form of explainability.

Model performance was evaluated on an independent test set, separate from the images used for training and validation. Standard object detection metrics were adopted, including precision (the proportion of correct predictions among all positive predictions), recall (the proportion of correct predictions among all actual instances), and mean Average Precision (mAP), calculated both at an Intersection over Union (IoU) threshold of 0.5 (mAP@0.5) and across thresholds from 0.5 to 0.95 (mAP@0.5:0.95). The IoU metric, defined as the ratio between the area of overlap and the total area covered by the predicted and ground truth bounding boxes, was used to determine the correctness of predictions according to the following formula:

$$IoU = \text{Areaofoverlap} / \text{Areaofunion}$$

Operational thresholds were set for prediction confidence (0.25) and IoU (0.6), in order to balance sensitivity and specificity in defect detection. The evaluation included both a quantitative analysis of the metrics and a qualitative review of the predictions, with particular attention to the challenges encountered in detecting small or atypically shaped defects.

Results

On the test set, the model demonstrated a varied ability to detect the different types of periodontal defects (Table 2). The overall precision, which reflects the proportion of correctly identified defects among all detections, was 0.592. The overall recall, indicating the proportion of actual defects correctly

Table 2 – Performance results of the YOLOv8 Model on the test set

Class	Precision	Recall	mAP@0.5	mAP@0.5:0.95
1	0.600	0.333	0.400	0.157
2+	0.518	0.508	0.495	0.205
Crater	0.581	0.444	0.541	0.209
Furcation	0.669	0.455	0.577	0.206
All	0.592	0.435	0.504	0.194

1: 1 wall defect; 2+: 2 or 3 walls defects; Crater: crater-shaped interproximal bone resorption; Furcation: furcation defects.

detected by the system, was 0.435. The mean Average Precision at an IoU threshold of 0.5 (mAP@0.5) reached 0.504, while the more stringent mAP averaged over IoU thresholds from 0.5 to 0.95 (mAP@0.5:0.95) was 0.194. In addition to the standard metrics we reported, we evaluated the detector at a lower IoU threshold (0.25) on the test set. We obtain mAP@0.25 = 0.555, thus not very different compared with mAP@0.5 = 0.504.

A breakdown by defect class revealed differences in detection performance. For furcation involvements, the model achieved the highest precision (0.669) and a recall of 0.455, with a mAP@0.5 of 0.577. Crater-like defects were detected with a precision of 0.581 and a recall of 0.444 (mAP@0.5: 0.541). The model's performance for vertical defects with 2 or more remaining walls was moderate (precision 0.518, recall 0.508, mAP@0.5: 0.495), while detection of 1-wall defects proved more difficult, with lower recall (0.333) and mAP (0.400 at IoU 0.5). Notably, the 1-wall defect class had the lowest recall (and precision), which corresponds to this class being the least represented in the training data.

Qualitative analysis of the model's predictions confirmed these trends. The system was generally able to correctly identify the location and type of more extensive and radiographically evident defects. However, false positives were observed, especially in areas with overlapping anatomical structures or radiographic artifacts, and false negatives were more common for defects with atypical morphology or limited size. These limitations are likely related to the inherent complexity of periodontal bone defect visualisation in 2-dimensional radiographs, as well as to the class imbalance present in the dataset.

Discussion

This study explored the feasibility of using a deep learning-based object detection model to automatically detect and classify periodontal osseous defects on standard intraoral radiographs. The model was trained to recognise 4 clinically relevant categories—1-wall defects, 2-or-more-wall defects, crater-like defects, and furcation involvements—based on expert-annotated periapical images. This approach aimed to assess whether AI systems can support the diagnostic workflow in periodontology by providing consistent and morphology-aware radiographic interpretation.

The mean Average Precision at an IoU threshold of 0.5 (mAP@0.5) reached 0.504, indicating that the model can identify a substantial proportion of clinically relevant periodontal bone defects. However, with a precision of around 0.59 and a recall of 0.43, the tool's accuracy is not yet sufficient for clinical use. It is important to contextualise these metrics from a clinical standpoint. In practice, a diagnostic aid would likely need to achieve much higher accuracy (eg, both precision and recall well above 0.8) to be considered reliable. These results should be viewed as a proof-of-concept; significantly higher performance (closer to experienced clinicians' accuracy) would be required for a diagnostic application. Thus, while the mAP of 0.50 demonstrates the model's learning capability, it is not sufficient for clinical adoption at this stage. Additional analysis at a relaxed IoU threshold (mAP@0.25 = 0.555)

showed only a modest performance gain, suggesting that localisation accuracy is not the primary limiting factor. Rather, the main constraints appear to be missed detections and occasional misclassification, particularly for the most difficult defect category. In other words, performance bottlenecks are more often related to whether and what the model detects, rather than how precisely it draws the bounding box. Given the small size and ill-defined borders of many periodontal defects, we acknowledge that exact box placement is often arbitrary, and that correct classification is likely to be more clinically meaningful than tight spatial localisation.

The highest precision was achieved with furcation and crater defects, these findings indicate that the system is more effective in identifying well-defined and larger defects, such as furcation involvements, whereas smaller or less distinct defects, particularly 1-wall vertical defects, are more frequently missed or inaccurately localised.

In recent years, the application of artificial intelligence (AI) to periodontal diagnostics has accelerated rapidly, driven by the widespread adoption of deep neural networks and increasing interest in automating diagnostic workflows. Many of the most influential studies in this field have focused on panoramic radiographs (OPG), exploiting the broad field of view of these images to assess bone loss across the entire dentition. While models developed on OPGs, such as U-Net, Mask R-CNN, and other custom networks, have demonstrated commendable accuracy in bone loss staging and in classifying periodontitis according to the 2018 guidelines,²⁶ these techniques lack the level of detail needed to characterise individual defects and are less sensitive when detecting localised defects, particularly in posterior regions and furcation areas.^{22,24,27,28} Most of these studies are limited to binary classifications (presence/absence of bone loss) or to identifying the general stage of disease, while research on specific defect morphologies remains scarce.¹⁹

Conversely, the use of periapical radiographs represents a more focused and detailed approach, particularly suited for analysing the morphological characteristics of bone defects. Recent studies employing this modality, such as Mao et al.,²³ have demonstrated the effectiveness of CNNs in detecting furcation defects with high levels of accuracy. Nevertheless, these works often limit their focus to specific defect types (eg, furcations only), and the diagnostic analysis remains confined to less articulated tasks compared to the complex variety of periodontal defects. Other models applied to periapical radiographs, such as multitask InceptionV3²⁹ and “hourglass” architectures,³⁰ have mainly concentrated on the quantitative measurement of bone loss or on distinguishing between mild and severe forms, without delving into detailed morphological differentiation. At the same time, the introduction of end-to-end workflows and multimodal models, including DualFit and other architectures integrating radiographic and textual data via NLP, has opened interesting avenues for automated clinical staging, although these approaches have yet to address the specific problem of defect-type identification.^{18,27}

Against this backdrop, our study stands out for several original contributions and added value. By using periapical radiographs, we aimed to leverage improved site-specific detail compared to panoramic images. However, we

acknowledge that 2D radiographs cannot reliably capture full 3-dimensional morphology, particularly in the buccolingual dimension. Thus, while intraoral images allow classification of common patterns, some morphological uncertainty remains—especially for crater-type or contained defects with intact cortical plates.^{23,30} In contrast to prior studies that focused on detecting overall bone loss or isolated furcation involvement,^{19,23,24} our model attempts to distinguish multiple defect categories—1-wall, ≥ 2 -walls, crater, and furcation—based on radiographic morphology alone. To our knowledge, this is the first application of deep learning object detection to site-level morphological classification of periodontal defects on periapical radiographs. However, 2D imaging cannot resolve buccolingual morphology and may under-detect defects masked by intact cortical plates. Accordingly, full morphological classification remains uncertain on 2D images and requires clinical/surgical verification. Unlike much of the existing literature, our model does not confine itself to general staging or binary discrimination; rather, it aims for fine-grained classification of different types of bone loss, reliably and automatically distinguishing between vertical defects, multi-wall defects, and furcation involvement. This level of diagnostic granularity marks a significant advance over previous models, which often only detected the presence or extent of bone loss without characterising its precise morphology.^{29,31}

From a technological standpoint, our study is also noteworthy for employing the YOLOv8 large architecture, an object-based detection strategy that, unlike classical segmentative or classificatory pipelines, enables rapid, localised, and potentially more robust identification of clinically relevant defects. In the landscape of YOLO-based studies in dental radiology, very few have explored this architecture, and generally for broader objectives such as diagnosing periodontitis or caries on bitewing images,¹⁹ never extending the analysis to the morphology of individual periodontal defects. This architectural choice also impacts the practical usability of the pipeline, which approaches real integration into daily workflows thanks to extremely fast inference times and an output format readily interpretable by clinicians.³¹

Another strength of our study concerns the clinical utility of the generated data: the ability to distinguish between categories such as vertical defects and furcation involvement is not only a technically relevant result but also provides genuine decision support for clinicians—guiding the selection of candidates for regenerative procedures and identifying therapeutic challenges with higher accuracy, as highlighted by several recent systematic reviews and clinical trials.^{22,32} In summary, our contribution addresses a distinct gap in the international literature, expanding the capabilities of AI systems for periodontal diagnosis from simple quantitative or staging evaluation to comprehensive morphological characterisation—a key prerequisite for personalised medicine and advanced treatment planning.

However, this study has several limitations. First, the dataset of 581 radiographs, while the maximum we could obtain with confirmed defects and adequate for a proof-of-concept study, is relatively small for a deep learning task with 4 classes. This limited quantity of training data may have restricted the model’s ability to capture the full

variability of defect presentations, thereby impacting its robustness. Moreover, the radiographs were all obtained from a single institution using the same imaging system. This homogeneity may limit the model's generalisability; the algorithm could be attuned to center-specific imaging features, raising the risk of overfitting. Validation on external datasets from different populations and radiographic equipment is needed to ensure broader applicability. Although the model was able to classify defects into 4 categories, the imbalance in class representation—particularly the relative scarcity of 1-wall defects—may have influenced performance. We did not implement specific measures (eg, oversampling or loss weighting) to counter this imbalance, which likely contributed to the model's difficulty in detecting the minority class. Addressing this in future research (through data augmentation or specialised training strategies) may improve performance. The use of 2-dimensional radiographs imposes inherent constraints in assessing 3-dimensional anatomical structures, particularly in cases of buccolingual defects or overlapping anatomical features. As demonstrated in previous studies,^{33,34} the exact morphology and number of remaining bony walls cannot be reliably determined from 2D radiographs. Our reference standard therefore reflects a radiographic consensus rather than true anatomical ground truth. Consequently, the model is inherently limited by the same diagnostic constraints and subjectivity affecting clinician interpretation, and its outputs should be understood as reproducing radiographic appearances rather than accurately reconstructing underlying 3-dimensional defect morphology. While periapical images allow reasonably accurate discrimination between 1-wall and multi-wall defects (hence the classification into “1” and “2+” categories) the exact number of remaining walls (eg, 2 vs 3) cannot be reliably inferred from radiographic grayscale alone. Such distinctions often require direct intraoperative assessment. In fact, certain defects initially interpreted as 1-wall based on radiographic appearance may later reveal additional residual walls upon flap reflection. Although 3-dimensional imaging modalities like cone-beam computed tomography (CBCT) could, in theory, improve anatomical characterisation, their routine use in periodontal diagnosis is not justified due to radiation exposure, cost, and limited clinical applicability in this context. Thus, any AI model trained on periapical images must necessarily operate within these intrinsic anatomical and imaging constraints. Our labels constitute a radiographic (2D) consensus rather than surgical/CBCT ground truth; therefore, the model's outputs should be interpreted as radiographic assistance within the initial diagnostic workflow, consistent with ALARA and current periodontal practice. Furthermore, our validation was performed on a hold-out portion of the same dataset; no independent external test was conducted. This lack of external or prospective validation limits the strength of our conclusions regarding clinical applicability.

As there are no published models addressing the exact task of defect-type classification on periapical radiographs, direct performance comparison is not available. We recognise this as a limitation and an area for future work (eg, testing alternative architectures or comparing against clinician readings).

While challenges remain, the findings underscore the potential of AI-assisted systems to support radiographic diagnosis of periodontal bone loss. The model's capacity to identify a range of clinically relevant defect types—even with moderate sensitivity—suggests that such tools could function as useful adjuncts in clinical workflows, contributing to more consistent and efficient defect detection and choice of therapy after periodontal re-evaluation.³⁵ Future enhancements, including the expansion of training datasets, optimisation of augmentation techniques, and exploration of alternative model architectures, are likely to further improve accuracy and generalisability.

Conclusion

This study demonstrated the feasibility of using a deep learning-based object detection model to identify and classify periodontal infrabony and furcation defects on standard intraoral radiographs. By distinguishing between clinically relevant defect morphologies, the model offers a proof of concept for AI-assisted tools that could support periodontal diagnosis and treatment planning. Although current performance is limited by dataset constraints, class imbalance, and the intrinsic limitations of 2-dimensional imaging, the results highlight the potential clinical utility of such systems. Further developments—such as expanding annotated datasets, refining model architectures, and validating performance in prospective, real-world settings—will be essential to translate these technologies into effective diagnostic support tools in daily periodontal practice. Future studies with larger and more varied radiographic datasets are needed to improve the model's accuracy and reliability, and should validate the model on external datasets or in a prospective clinical study to confirm its diagnostic performance and generalisability.

Funding

No funds were received for the realisation of this study.

Author contribution

NAV: conceived the study, conducted the radiographic image annotation, wrote the manuscript, and supervised all clinical aspects of the work. LMA: selected and organised the radiographic dataset and contributed to image annotation. FC: provided supervision for the technical and engineering components of the study. SM: co-designed the study, developed the research protocol, and performed the data analysis and statistical evaluation

Conflict of interest

None disclosed.

Data availability statement

The data supporting this study's findings are available from the corresponding author upon reasonable request.

B I B L I O G R A P H Y

- Kaldahl WB, Kalkwarf KL, Patil KD, Dyer JK, Bates RE. Evaluation of four modalities of periodontal therapy. *J Periodontol* 1988;59:783–93. doi: [10.1902/jop.1988.59.12.783](https://doi.org/10.1902/jop.1988.59.12.783).
- Becker W, Becker BE, Caffesse R, et al. A longitudinal study comparing scaling, osseous surgery, and modified widman procedures: results after 5 years. *J Periodontol* 2001;72:1675–84. doi: [10.1902/jop.2001.72.12.1675](https://doi.org/10.1902/jop.2001.72.12.1675).
- Caffesse RG, Sweeney PL, Smith BA. Scaling and root planing with and without periodontal flap surgery. *J Clin Periodontol* 1986;13:205–10. doi: [10.1111/j.1600-051x.1986.tb01461.x](https://doi.org/10.1111/j.1600-051x.1986.tb01461.x).
- Prichard JF. The etiology, diagnosis and treatment of the intrabony defect. *J Periodontol* 1967;38:455–65. doi: [10.1902/jop.1967.38.6_part1.455](https://doi.org/10.1902/jop.1967.38.6_part1.455).
- Melcher AH. On the repair potential of periodontal tissues. *J Periodontol* 1976;47:256–60. doi: [10.1902/jop.1976.47.5.256](https://doi.org/10.1902/jop.1976.47.5.256).
- Nyman S, Lindhe J, Karring T, Rylander H. New attachment following surgical treatment of human periodontal disease. *J Clin Periodontol* 1982;9:290–6. doi: [10.1111/j.1600-051X.1982.tb02095.x](https://doi.org/10.1111/j.1600-051X.1982.tb02095.x).
- Clementini M, Ambrosi A, Ciccirelli V, De Risi V, de Sanctis M. Clinical performance of minimally invasive periodontal surgery in the treatment of infrabony defects: Systematic review and meta-analysis. *J Clin Periodontol* 2019;46:1236–53. doi: [10.1111/jcpe.13201](https://doi.org/10.1111/jcpe.13201).
- Nibali L, Koidou VP, Nieri M, Barbato L, Pagliaro U, Cairo F. Regenerative surgery versus access flap for the treatment of intra-bony periodontal defects: a systematic review and meta-analysis. *J Clin Periodontol* 2020;47:320–51. doi: [10.1111/jcpe.13237](https://doi.org/10.1111/jcpe.13237).
- Cortellini P, Cortellini S, Bonaccini D, Tonetti MS. Modified minimally invasive surgical technique in human intrabony defects with or without regenerative materials—10-year follow-up of a randomized clinical trial: Tooth retention, periodontitis recurrence, and costs. *J Clin Periodontol* 2022;49:528–36. doi: [10.1111/jcpe.13627](https://doi.org/10.1111/jcpe.13627).
- Meyle J, Hoffmann T, Topoll H, et al. A multi-centre randomized controlled clinical trial on the treatment of intra-bony defects with enamel matrix derivatives/synthetic bone graft or enamel matrix derivatives alone: Results after 12 months. *J Clin Periodontol* 2011;38:652–60. doi: [10.1111/j.1600-051X.2011.01726.x](https://doi.org/10.1111/j.1600-051X.2011.01726.x).
- Sculean A, Pietruska M, Arweiler NB, Aushill TM, Nemcovsky C. Four-year results of a prospective-controlled clinical study evaluating healing of intra-bony defects following treatment with an enamel matrix protein derivative alone or combined with a bioactive glass. *J Clin Periodontol* 2007;34:507–13. doi: [10.1111/j.1600-051X.2007.01084.x](https://doi.org/10.1111/j.1600-051X.2007.01084.x).
- Tavelli L, Chen CY, Barootchi S, Kim DM. Efficacy of biologics for the treatment of periodontal infrabony defects: An American Academy of Periodontology best evidence systematic review and network meta-analysis. *J Periodontol* 2022;93:1803–26. doi: [10.1002/JPER.22-0120](https://doi.org/10.1002/JPER.22-0120).
- Sanz M, Herrera D, Kerschull M, et al. Treatment of stage I-III periodontitis—the EFP S3 level clinical practice guideline. *J Clin Periodontol* 2020;47:4–60. doi: [10.1111/jcpe.13290](https://doi.org/10.1111/jcpe.13290).
- Valente NA, Pileri C, Floris L, Carrus N, Natto Z, Clementini M. Clinical outcomes of periodontal regeneration using biologic agents alone or in combination with graft materials for intrabony defects: a systematic review and meta-analysis. *J Dent* 2025;162. doi: [10.1016/j.jdent.2025.106080](https://doi.org/10.1016/j.jdent.2025.106080).
- Nibali L, Sultan D, Arena C, Pelekos G, Lin GH, Tonetti M. Periodontal infrabony defects: Systematic review of healing by defect morphology following regenerative surgery. *J Clin Periodontol* 2021;48:100–13. doi: [10.1111/jcpe.13381](https://doi.org/10.1111/jcpe.13381).
- Papapanou PN, Tonetti MS. Diagnosis and epidemiology of periodontal osseous lesions. *Periodontol* 2000;22:8–21. doi: [10.1034/j.1600-0757.2000.2220102.x](https://doi.org/10.1034/j.1600-0757.2000.2220102.x).
- Reynolds MA, Kao RT, Nares S, et al. Periodontal regeneration — intrabony defects: practical applications from the AAP Regeneration Workshop. *Clin Adv Periodontics* 2015;5:21–9. doi: [10.1902/cap.2015.140062](https://doi.org/10.1902/cap.2015.140062).
- Xu P, Gholamalizadeh T, Moshfeghifar F, Darkner S, Erleben K. Deep-learning-based segmentation of individual tooth and bone with periodontal ligament interface details for simulation purposes. *IEEE Access* 2023;11:102460–70. doi: [10.1109/ACCESS.2023.3317512](https://doi.org/10.1109/ACCESS.2023.3317512).
- Li KC, Mao YC, Lin MF, et al. Detection of tooth position by YOLOv4 and various dental problems based on CNN with bite-wing radiograph. *IEEE Access* 2024;12:11822–35. doi: [10.1109/ACCESS.2023.3348788](https://doi.org/10.1109/ACCESS.2023.3348788).
- Samaranayake L, Tuygunov N, Schwendicke F, et al. The transformative role of artificial intelligence in dentistry: a comprehensive overview. Part 1: Fundamentals of AI, and its contemporary applications in dentistry. *Int Dent J* 2025;75:383–96. doi: [10.1016/j.identj.2025.02.005](https://doi.org/10.1016/j.identj.2025.02.005).
- Tuygunov N, Samaranayake L, Khurshid Z, et al. The transformative role of artificial intelligence in dentistry: a comprehensive overview part 2: the promise and perils, and the international dental federation communique. *Int Dent J* 2025;75:397–404. doi: [10.1016/j.identj.2025.02.006](https://doi.org/10.1016/j.identj.2025.02.006).
- Kurt-Bayrakdar S, Bayrakdar İŞ, Yavuz MB, et al. Detection of periodontal bone loss patterns and furcation defects from panoramic radiographs using deep learning algorithm: a retrospective study. *BMC Oral Health* 2024;24. doi: [10.1186/s12903-024-03896-5](https://doi.org/10.1186/s12903-024-03896-5).
- Mao YC, Huang YC, Chen TY, et al. Deep learning for dental diagnosis: a novel approach to furcation involvement detection on periapical radiographs. *Bioengineering* 2023;10. doi: [10.3390/bioengineering10070802](https://doi.org/10.3390/bioengineering10070802).
- Krois J, Ekert T, Meinhold L, et al. Deep learning for the radiographic detection of periodontal bone loss. *Sci Rep* 2019;9. doi: [10.1038/s41598-019-44839-3](https://doi.org/10.1038/s41598-019-44839-3).
- Tejani AS, Klontzas ME, Gatti AA, et al. Checklist for Artificial Intelligence in Medical Imaging (CLAIM): 2024 update. *Radiol Artif Intell* 2024;6:e240300. doi: [10.1148/ryai.240300](https://doi.org/10.1148/ryai.240300).
- G Caton J, Armitage G, Berglundh T, et al. A new classification scheme for periodontal and peri-implant diseases and conditions - Introduction and key changes from the 1999 classification. *J Clin Periodontol* 2018;45:S1–8. doi: [10.1111/jcpe.12935](https://doi.org/10.1111/jcpe.12935).
- Xue T, Chen L, Sun Q. Deep learning method to automatically diagnose periodontal bone loss and periodontitis stage in dental panoramic radiograph. *J Dent* 2024;150. doi: [10.1016/j.jdent.2024.105373](https://doi.org/10.1016/j.jdent.2024.105373).
- Ertaş K, Pence I, Casmeli MS, Ay ZY. Determination of the stage and grade of periodontitis according to the current classification of periodontal and peri-implant diseases and conditions (2018) using machine learning algorithms. *J Periodontal Implant Sci* 2022;52. doi: [10.5051/JPIS.2201060053](https://doi.org/10.5051/JPIS.2201060053).
- Chang J, Chang MF, Angelov N, et al. Application of deep machine learning for the radiographic diagnosis of periodontitis. *Clin Oral Investig* 2022;26:6629–37. doi: [10.1007/s00784-022-04617-4](https://doi.org/10.1007/s00784-022-04617-4).
- Danks RP, Bano S, Orishko A, et al. Automating Periodontal bone loss measurement via dental landmark localisation. *Int J Comput Assist Radiol Surg* 2021;16:1189–99. doi: [10.1007/s11548-021-02431-z](https://doi.org/10.1007/s11548-021-02431-z).

31. Cerda Mardini D, Cerda Mardini P, Vicuña Iturriaga DP, Ortuño Borroto DR. Determining the efficacy of a machine learning model for measuring periodontal bone loss. *BMC Oral Health* 2024;24. doi: [10.1186/s12903-023-03819-w](https://doi.org/10.1186/s12903-023-03819-w).
32. Mao K, Thu KM, Hung KF, Yu OY, Hsung RT-C, Lam WY-H. Artificial intelligence in detecting periodontal disease from intraoral photographs: a systematic review. *Int Dent J* 2025;75:100883. doi: [10.1016/j.identj.2025.100883](https://doi.org/10.1016/j.identj.2025.100883).
33. Zengin AZ, Sumer P, Celenk P. Evaluation of simulated periodontal defects via various radiographic methods. *Clin Oral Investig* 2015;19:2053–8. doi: [10.1007/s00784-015-1421-8](https://doi.org/10.1007/s00784-015-1421-8).
34. Gomes-Filho IS, Sarmiento VA, De Castro MS, et al. Radiographic features of periodontal bone defects: evaluation of digitized images. *Dentomaxillofac Radiol* 2007;36:256–62. doi: [10.1259/dmfr/25386411](https://doi.org/10.1259/dmfr/25386411).
35. Paternò Holtzman L, Valente NA, Vittorini Orgeas G, Copes L, Discepoli N, Clementini M. Change in clinical parameters after subgingival instrumentation for the treatment of periodontitis and timing of periodontal re-evaluation: a systematic review and meta-analysis. *J Clin Periodontol* 2025;52:137–58. doi: [10.1111/jcpe.13985](https://doi.org/10.1111/jcpe.13985).